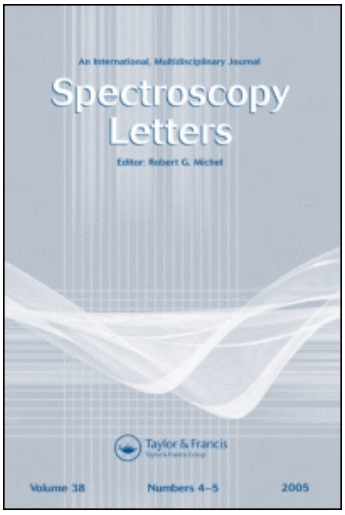

Spectroscopy Letters
Publication details, including instructions for authors and subscription information:
http://www.informaworld.com/smpp/title~content=t713597299

A WAVELET PACKETS TECHNIQUE FOR THE DETECTION OF ANOMALIES IN FOURIER TRANSFORM INFRARED INTERFEROGRAMS

Falih H. Ahmad[a]; Ray M. Castellane[b]; Bartley P. Durst[b]
[a] Department of Engineering Technology, The University of North Carolina Charlotte, NC, U.S.A. [b] Department of The Army, Engineer Research and Development Center, Vicksburg, MS, U.S.A.

Online publication date: 14 August 2002

To cite this Article Ahmad, Falih H. , Castellane, Ray M. and Durst, Bartley P.(2002) 'A WAVELET PACKETS TECHNIQUE FOR THE DETECTION OF ANOMALIES IN FOURIER TRANSFORM INFRARED INTERFEROGRAMS', Spectroscopy Letters, 35: 4, 527 — 541
To link to this Article: DOI: 10.1081/SL-120013889
URL: http://dx.doi.org/10.1081/SL-120013889

MARCEL DEKKER, INC. • 270 MADISON AVENUE • NEW YORK, NY 10016

SPECTROSCOPY LETTERS, 35(4), 527–541 (2002)

A WAVELET PACKETS TECHNIQUE FOR THE DETECTION OF ANOMALIES IN FOURIER TRANSFORM INFRARED INTERFEROGRAMS

Falih H. Ahmad,[1,*] Ray M. Castellane,[2] and Bartley P. Durst[2]

[1]Department of Engineering Technology,
The University of North Carolina Charlotte, NC 28223
[2]Department of The Army, Engineer Research and
Development Center, Waterways Experiment Station,
3909 Halls Ferry Road, Vicksburg, MS 39180-6199

ABSTRACT

A technique that integrates applications of wavelet packets and principal component analysis is developed. This technique is applied for the purpose of detecting anomalies in Fourier Transform Infrared (FTIR) interferograms. An experimental example is given to demonstrate the performance of this technique.

Key Words: Wavelets; Interferogram; Fourier transform; Infrared spectroscopy

*Corresponding author. Fax: (704) 510-6499; E-mail: fhahmad@uncc.edu

INTRODUCTION

In recent years, wavelets have found their way into many different fields of science and engineering. Wavelets constitute a family of functions constructed from dilation and translation of a single function called the mother wavelet. They possess several useful properties, such as orthogonality, compact support, and exact representation of polynomials to a certain degree. Also, they are able to produce localization in the wavelength and frequency domains, locate and identify significant events, detect and localize various types of disturbances and to represent functions at different levels of resolution (i.e., multiresolution).[1] For example, wavelet multiresolution analysis is applied to the solution of a magnetic inverse problem and used to obtain a good estimation of the permeability profile,[2] and the production of best image fusion.[3] Furthermore, best wavelet bases are used for the compression of magnetic resonance images,[4] delay and Doppler estimation,[5] and implementation of a time-varying matched filter and its application to the inverse synthetic aperture radar.[6] An entropy-based algorithm for best wavelet basis selection is presented in,[7] and alternatively a method that is based on rate-distortion sense is developed in[8] for the selection of best wavelet packet bases.

In the applications of spectroscopy for monitoring chemical processes and calibration of chemical systems, an understanding of the various chemical process mechanisms and measurement procedures that contribute to the analysis and implementation of such processes and system performance is important. Accordingly, statistical multivariate approaches have been developed for and utilized in such applications.[9–15] In particular, multivariate approaches are used to achieve reductions in spectral noise levels,[9] detect instrument variations,[12] identify sources and natures of spectral disturbances,[13,14] and detect sensor faults.[15] Furthermore, the advantage in using multivariate approaches is seen when a principal component analysis (PCA), which is a statistical multivariate approach, is used to treat all process variables simultaneously. In this case many of the limitations of classical statistical processes such as the ones presented in[16] are circumvented.[10,11] PCA is a technique that transforms a number of related variables to a set of uncorrelated variables. It can be used as a data reduction technique and a diagnostic tool or a control device.[12] Moreover, PCA is performed in the wavelets domain to improve spectral features classification,[17] and to detect and identify spectral anomalies due to material aging.[18] It is concluded in[18] that the integration of wavelet processing with techniques from multivariate statistical process control provides a useful means of localizing, detecting, and identifying spectral disturbances.

Analyses of interferograms are performed for many scientific benefits. For example, these analyses are used to determine the optical constant of a thin film,[19] to measure surface depth at nanometer scales,[20] to retrieve the refractive-index of fibers[21] and for the measurement of atomic oscillator strengths and atomic energy level populations.[22] The analysis of the interferograms is performed using Fourier transform,[20,22] Green's function,[23] an error function,[24] a phase-resolved correlation method[25] and a wavelet method.[26]

In conjunction with the methods of identifying spectral disturbances, a technique is proposed in this article. This technique utilizes wavelet packets and PCA to identify the presence of anomalies in interferograms.

The sections of this article are organized as follows: A summary about wavelet packets is given in Sec. 2. The proposed technique is outlined in Sec. 3. In Sec. 4, an experimental example is given to illustrate the performance of the proposed technique.

Wavelet Packets

Wavelet packets are a generalized family of multiresolution orthogonal or biorthogonal basis that include wavelets. The wavelet packet method is a generalization of wavelet decomposition that offers a richer range of possibilities for signal analysis. In wavelet analysis, a signal is split into an approximation and a detail. The approximation is then itself split into a second-level approximation and detail, and the process is repeated. For an n-level decomposition, there are $n+1$ possible ways to decompose a signal. In wavelet packet analysis, the details as well as the approximations can be split. This yields more than $2^{2^{n-1}}$ different ways of decomposition and, as a result, a wavelet packet decomposition tree is developed.[4] Several cost functions are useful for the development of the best decomposition tree for a given signal, and one of the most attractive is Shannon entropy.[7] All families of wavelets are applicable in the technique that is proposed in this article, examples of such families are,[4]:

- Daubechies wavelets with family members: *db*1-*db*10
- Symlets wavelets with family members: *sym*2-*sym*8
- Coiflets wavelets with family members: *coif* 1-*coif* 5
- A discrete approximation of Meyer wavelets
- Haar wavelets

Moreover, using Shannon entropy, an algorithm for developing the best decomposition tree for a signal (S) is utilized by the technique that is presented in this article. This algorithm is as follows:[7]

(a) Choose l as the maximum number of levels of decomposition.
(b) While the level of decomposition is less than l, do the following:

- Let the jth signal at the ith level be $S_{i,j}$, calculate Shannon entropy of this signal, $\eta(S_{i,j}), i < l$.
- Decompose $S_{i,j}$ into two signals, $S_{i+1,q}$ and $S_{i+1,k}$, and compute their corresponding Shannon entropy, $\eta(S_{i+1,q})$ and $\eta(S_{i+1,k})$, $i+1 < l$.
- If $\eta(S_{i,j}) > \eta(S_{i+1,q}) + \eta(S_{i+1,k})$ then retain $S_{i+1,q}$ and $S_{i+1,k}$, continue decomposing. Otherwise retain $S_{i,j}$ and stop.

An example of a best decomposition tree for S is shown in Fig. 1. The branching or non-branching of every signal in this tree is dictated by Shannon entropy. Computation of Shannon entropy has permitted the branching of the signal $S_{1,1}$ to $S_{2,1}$ and $S_{2,2}$, however, it did not permit the branching of the signal $S_{2,1}$.

Interferograms Analysis Technique

For the purpose of presenting the proposed technique we consider, A, a set of FTIR interferograms of a given pure material. In addition, we

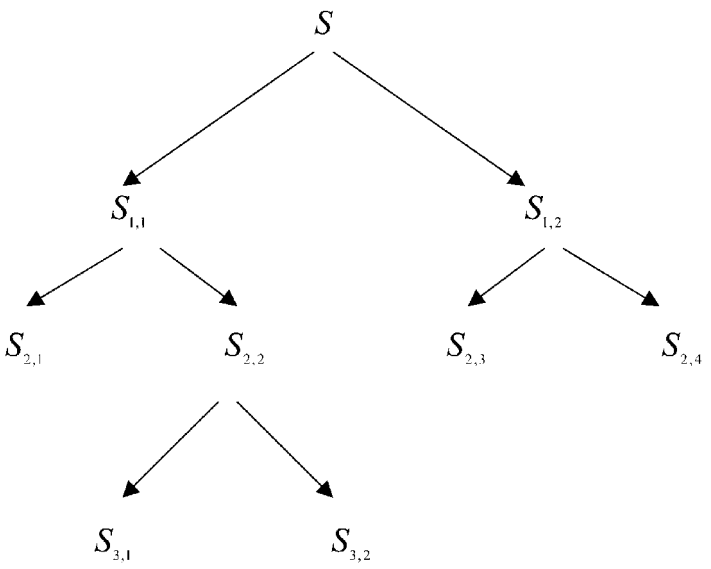

Figure 1. Example of best decomposition tree for a signal S.

assume that these interferograms are with no anomalies and they are generated independently [model interferograms[18]]. This set is represented as:

$$A = \{I1, I2, \ldots, I\mathrm{N}\} \tag{1}$$

where the total number of the members in this set is "N" and *Ii* represents the *i*th interferogram in this set. In addition, we consider the set *B* as:

$$B = \{It\} \tag{2}$$

where *It* is the only member in this set. *It* is a FTIR interferogram representing the same material, however, tested for minute anomalies due to contaminations [tested interferogram[18]]. Accordingly, the proposed technique for the analysis of interferograms is outlined as follows:

3.1

Any one of the families of wavelets listed in Sec. 2, along with the Shannon entropy algorithm outlined in the same section, is used to generate the corresponding best decomposition trees for the members of the sets *A* and *B*. Without loss of generality, let Coiflets wavelet (*coif*1-*coif* 5) be the family that is utilized. The first family member, *coif*1, is applied first to $I1, I2, \mathrm{K}, I\mathrm{N}$ and *It*. The resulting best decomposition trees and their corresponding signals are listed symbolically in Table 1. In this table, the subscripts in the symbols of the best decomposition trees (first column) indicate correspondence to interferograms on which the decompositions were performed. The superscripts in the symbols of the decomposed signals

Table 1. Symbolic Listing of Best Decomposition Trees and Their Corresponding Branching Packet Signals

Best Decomposition Tree	Branching *j*th Signals at the *i*th Decomposition Level
$coif1BDT_{I1}$	$coif1S^{I1}_{i1,j1}$, $i1 = 1,2,3,\ldots,\ j1 = 1,2,3,\ldots$
$coif1BDT_{I2}$	$coif1S^{I2}_{i2,j2}$, $i2 = 1,2,3,\ldots,\ j2 = 1,2,3,\ldots$
$coif1BDT_{I3}$	$coif1S^{I3}_{i3,j3}$, $i3 = 1,2,3,\ldots,\ j3 = 1,2,3,\ldots$
⋮	⋮
$coif1BDT_{IN}$	$coif1S^{IN}_{iN,jN}$, $iN = 1,2,3,\ldots,\ jN = 1,2,3,\ldots$
$coif1BDT_{It}$	$coif1S^{It}_{it,jt}$, $it = 1,2,3,\ldots,\ jt = 1,2,3,\ldots$

(second column) indicate correspondence of these signals to interferograms on which the decompositions were performed. The first subscripts in the symbols of the decomposed signals are decomposition levels and the second subscripts are numerations of the decomposed signals.

3.2

Assuming that the first signals of the 1st row and the last row of Table 1, i.e., $coif1S_{1,1}^{I1}$ and $coif1S_{1,1}^{It}$, exist due to Shannon entropy, they are compared for branching or non-branching. If they behave similarly then they are ignored otherwise they are retained as a mismatched pair. This procedure is repeated for all the signals, which exist due to Shannon entropy, from the 1st row and their corresponding signals with same subscripts from the last row of Table 1 and all mismatched pairs are retained. These mismatched pairs are used to formulate a "mismatched" set, $R1mm$. This set is given symbolically as:

$$R1mm = \{mm1_1, mm1_2, mm1_3, \ldots, mm1_{R1M}\} \tag{3}$$

where $mm1_k$ is the kth member of the set and $R1M$ is the total number of the mismatched pairs. These mismatches represent dissimilarities between the model and tested interferograms and these dissimilarities are manifested in the wavelet domain through the multiresolution and localization properties of the wavelet packets. The same procedure is repeated for the 2nd, 3rd, 4th, ..., and the Nth row of Table 1 where for every row the corresponding mismatched set is formulated. These sets are represented symbolically as:

$$\begin{aligned} R2mm &= \{mm2_1, mm2_2, mm2_3, \ldots, mm2_{R2M}\}, \\ R3mm &= \{mm3_1, mm3_2, mm3_3, \ldots, mm3_{R3M}\}, \\ &\vdots \\ R\mathrm{N}mm &= \{mm\mathrm{N}_1, mm\mathrm{N}_2, mm\mathrm{N}_3, \ldots, mm\mathrm{N}_{R\mathrm{N}M}\}. \end{aligned}$$

Each element in sets $R1mm, R2mm, \mathsf{K}, R\mathrm{N}mm$ is a pair of mismatched signals. The indices of the signals of each pair are the same and they correspond to the jth signal at the ith tree level. The first signal of this pair corresponds to a model interferogram and the second corresponds to the tested interferogram. Next, only elements with the same indices that appear in all the sets $R1mm, R2mm, \ldots, R\mathrm{N}mm$ are retained and grouped. A symbolic presentation of the (i,j) group is:

$$G_{i,j} = \begin{bmatrix} \left(coif1S_{i,j}^{I1}, coif1S_{i,j}^{It}\right), \left(coif1S_{i,j}^{I2}, coif1S_{i,j}^{It}\right), \ldots, \\ \left(coif1S_{i,j}^{IN}, coif1S_{i,j}^{It}\right) \end{bmatrix} \tag{4}$$

Next, the first signals from each pair of signals in the group $G_{i,j}$ are used to form a set that corresponds to the model interferograms, symbolically this set is presented as:

$$set1_{i,j} = \left\{coif1S_{i,j}^{I1}, coif1S_{i,j}^{I2}, \ldots, coif1S_{i,j}^{IN}\right\} \tag{5}$$

and the arithmetic mean of all the second signals of the pair of signals in the group $G_{i,j}$ is computed and used to form a one element set that corresponds to the tested interferogram, symbolically this set is presented as:

$$set2_{i,j} = \left\{amcoif1S_{i,j}^{It}\right\} \tag{6}$$

3.3

The elements of the set $set1_{i,j}$ are used to develop a PCA model, $PCAcoif1S_{i,j}^{1}$.[12] This procedure is repeated for each developed group. As a result, a family of PCA models is developed which belongs to *coif*1. This family is named symbolically as $PCAcoif1S^{I}$. The number of the members of this family is equal to the number of the elements that have the same indices and appear in all the sets $R1mm, R2mm, \mathsf{K}, RNmm$. Each member from the family $PCAcoif1S^{I}$ is used to test for the existence of a localized anomaly in the tested interferogram.

3.4

Information from PCA model $PCAcoif1S_{i,j}^{1}$, which is a member of the $PCAcoif1S^{I}$ family, is used to test for existence of anomalies in the *j*th signal at the *i*th level of the best decomposition tree of the tested interferogram. This is performed as follows:

3.4.1

The Q-limit of the PCA model $PCAcoif1S_{i,j}^{1}$ is calculated using the following equations:[12,18]

$$\theta_1 = \sum_{q=r+1}^{p} l_q \tag{7}$$

$$\theta_2 = \sum_{q=r+1}^{p} l_q^2 \tag{8}$$

$$\theta_3 = \sum_{q=r+1}^{p} l_q^3 \tag{9}$$

$$h_0 = 1 - \frac{2\theta_1\theta_3}{3\theta_2^2} \tag{10}$$

$$Q = \theta_1 \left[\frac{ch_0\sqrt{2\theta_2}}{\theta_1} + \frac{\theta_2 h_0(h_0 - 1)}{\theta_1^2} + 1 \right]^{1/h_0} \tag{11}$$

where Q is the Q-limit, c is an approximately normally distributed function with zero mean and unit variance and l_q is the qth eigenvalue of the $p \times p$ covariance matrix of $PCAcoif1S^I_{i,j}$ for which this limit is calculated.[12] In the process of principal component analysis *weights* are assigned to the eigenvalues of the covariance matrix.[12] These weights are used to discard r out of p eigenvalues,[12].

3.4.2

The principal components of $PCAcoif1S^1_{i,j}$ are used to compute its Q-Values.[12]

3.4.3

Values of the indices of $PCAcoif1S^1_{i,j}$ are used to select the corresponding signal from set $set2_{i,j}$ given in equation [6]. This signal is combined with $PCAcoif1S^1_{i,j}$ to form a modified version of $PCAcoif1S^1_{j,i}$ and labeled $MPCAcoif1S^1_{i,j}$.[12] The principal components of $MPCAcoif1S^1_{i,j}$ are used to compute its Q-Values.[12,18]

3.4.4

Q-values that were generated in steps 3.4.2 and 3.4.3 are compared with the Q-limit that was generated in step 3.4.1. Q-values that exceed this Q-limit are indications of existence of localized anomalies in the tested interferogram.[12]

3.4.5

Steps 3.4.1, 3.4.2, 3.4.3, and 3.4.4 are repeated for all family members of the PCA model $PCAcoif1S^I$ and their corresponding tested interferogram localized anomalies are identified.

3.5

Steps 3.2 and 3.3 are repeated and the PCA models $PCAcoif2S^I$, $PCAcoif3S^I$, $PCAcoif4S^I$ and $PCAcoif5S^I$ are generated.

3.6

Step 3.4 is repeated for all PCA models generated in step 3.5. As a result all localized anomalies for the tested interferogram are detected.

Experimental Example

A Nicolet 750 Fourier Transform Infrared spectrometer was used to generate 20 interferograms of pure acetone. These interferograms were labeled $I1, I2, \ldots, I20$. Five hundred parts per million of diesel fuel was added to this pure acetone, and the same spectrometer was used under the same conditions to generate an interferogram of the contaminated acetone. This interferogram was labeled It. The interferograms $I1$ and It are shown in Figs. 2 and 3, respectively. The proposed technique was applied and best decompostion trees were generated using the *Coiflets* wavelet family. For illustration, the best decomposition tree of $I1$ due to using *Coif*1, $coif1BDT_{I1}$, is shown in Fig. 4 and that of It, $coif1BDT_{It}$, is shown in Fig 5. It is noted from these two figures that the only mismatched pair of signals is $(coif1S^{I1}_{1,1}, coif1S^{It}_{1,1})$. Using *Coif*2, *Coif*3, *Coif*4, and *Coif*5, the corresponding best trees were generated. These trees and their corresponding

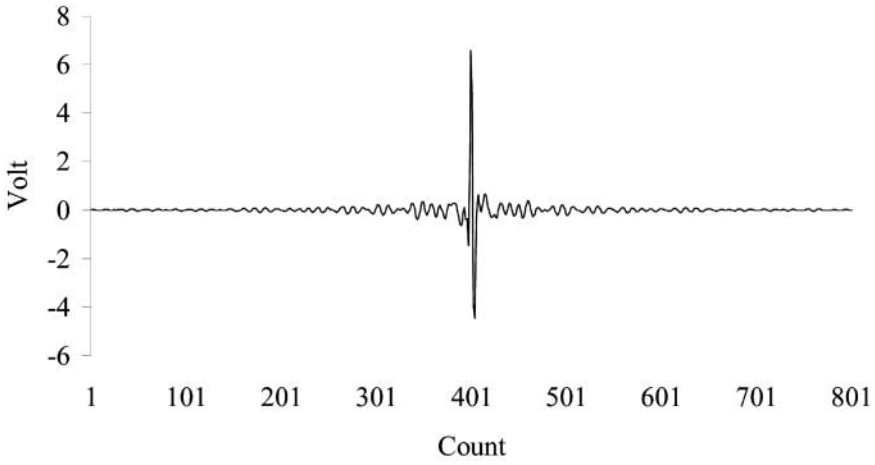

Figure 2. Interferogram of acetone with no anomalies.

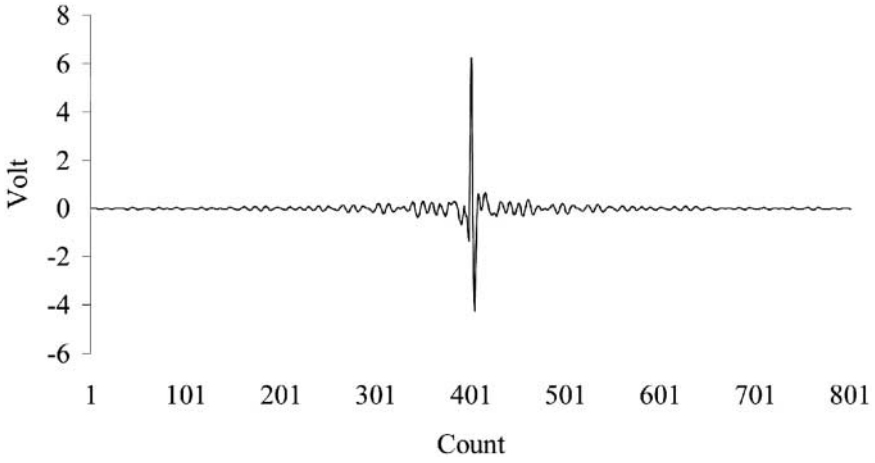

Figure 3. Interferogram of acetone with anomalies.

mismatched pairs of signals are listed symbolically in Table 2. Tables similar to Table 2 were generated for *I*2 through *I*20 along with *It*. In the case of the first wavelet packet family member, *coif*1, the signals $coif1S_{1,1}^{I1}$ through $coif1S_{1,1}^{I20}$ were used to develop the corresponding PCA model, $PCAcoif1S_{1,1}^{1}$ and equations [7] through [11] were used to calculate its Q-Limit.[12] Its

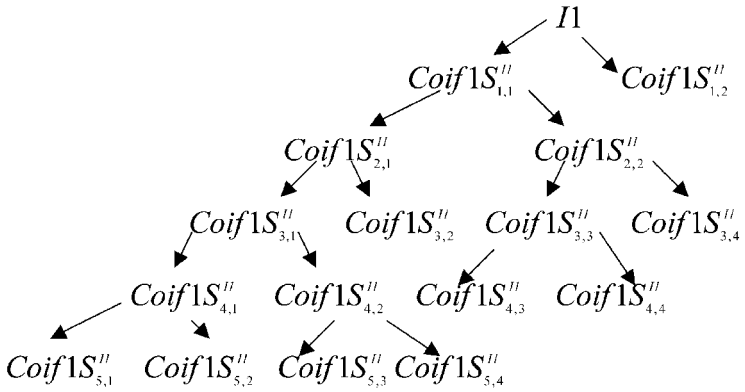

Figure 4. Best tree of $I1$ ($coif1BDT_{I1}$).

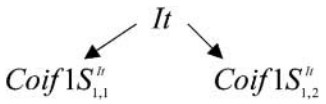

Figure 5. Best tree of It ($coif1BDT_{It}$).

Table 2. Mismatched Pairs of Signals from Best Decompostion Trees of $I1$ and It of the Experimental Example

Best Decomposition Trees	Mismatched Pairs of Signals
$coif2BDT_{I1}, coif2BDT_{It}$	$(coif2S^{I1}_{1,1}, coif2S^{It}_{1,1})$
$coif3BDT_{I1}, coif3BDT_{It}$	$(coif3S^{I1}_{1,1}, coif3S^{It}_{1,1})$, $(coif3S^{I1}_{2,4}, coif3S^{It}_{2,4})$, $(coif3S^{I1}_{3,6}, coif3S^{It}_{3,6})$, $(coif3S^{I1}_{4,7}, coif3S^{It}_{4,7})$ $(coif3S^{I1}_{4,8}, coif3S^{It}_{4,8})$
$coif4BDT_{I1}, coif4BDT_{It}$	$(coif4S^{I1}_{1,1}, coif4S^{It}_{1,1})$, $(coif4S^{I1}_{2,4}, coif4S^{It}_{2,4})$
$coif5BDT_{I1}, coif5BDT_{It}$	$(coif5S^{I1}_{1,1}, coif5S^{It}_{1,1})$, $(coif5S^{I1}_{3,6}, coif5S^{It}_{3,6})$ $(coif5S^{I1}_{3,8}, coif5S^{It}_{3,8})$

principal components were used to calculate its Q-Values.[12] Next, the arithmetic mean of the second signals from this mismatched pair, $amcoif1S^{It}_{1,1}$, was combined with this PCA model and $MPCAcoif1S_{1,1}$ was developed. Its principal components were computed and used to generate its

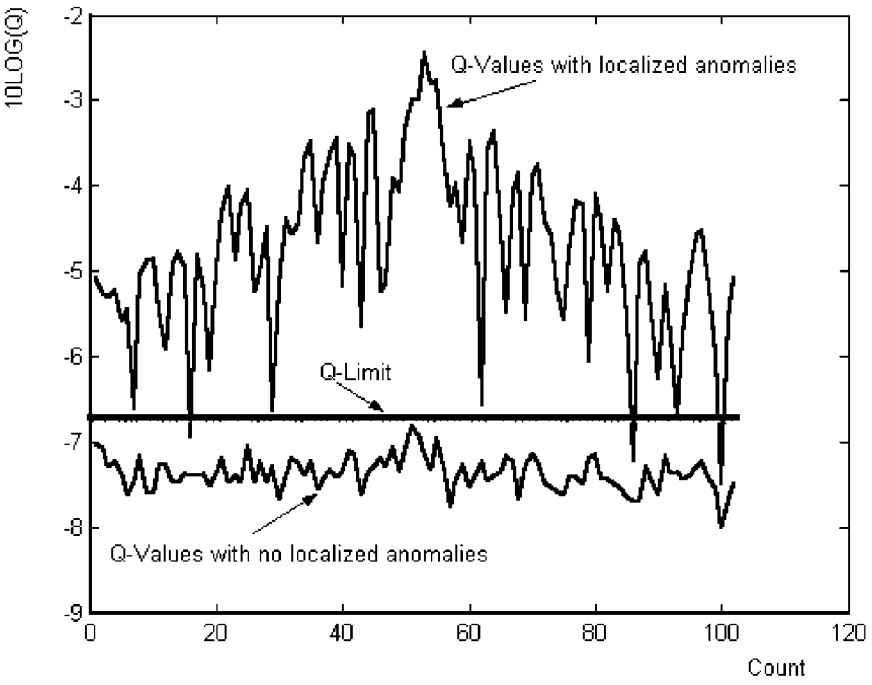

Figure 6. Q-Limit and Q-Values corresponding to $PCAcoif1S^{I}_{1,1}$ PCA model.

Q-Values.[12] The Q-limit and both Q-Values are shown in Fig. 6 where the detection of a localized anomaly is indicated. This procedure was repeated for every mismatched signal presented in Table 2 and plots similar to the one presented in Fig. 6 were produced for all localized anomalies.

CONCLUSION

Through an experimental example it is demonstrated that a technique proposed in this article that combines the applications of wavelet packets and principal component analysis provides a useful means for the detection of anomalies in interferograms. This technique makes use of the localization property of wavelet packets and Shannon entropy criterion where signal multiresolution decomposition is used to represent these interferograms. This technique is applicable to spectroscopy testing and measurements.

ACKNOWLEDGMENTS

The tests described and the resulting data presented herein, unless otherwise noted, were performed under contract DACA42-00-C-0048 from the Department of Defense, Engineering Research and Development Center, ERDC, Vicksburg, Mississippi, USA. The authors would like to extend their sincere thanks to Mrs. Pamela Kinnebrew, Chief, Survivability Engineering Branch, for making the Radiation Laboratory at the center available where all experiments were conducted. Permission was granted by the Chief of Engineers to publish this information.

REFERENCES

1. Kaiser, G. *A Friendly Guide to Wavelets*; Springer Verlag Publishing Company: 1994; 60–174.
2. Cho, J.-K.; Park, S.-B.; Lee, C.-H.; Jung, H.-K.; Hahn, S.-Y.; Koh, C.-S. Multiresolution Analysis for Permeability Reconstruction Using Wavelet. IEEE Transactions on Magnetics **1999**, *35* (5), 3757–3759.
3. Nunez, J.; Otazu, X.; Fors, O.; Prades, A.; Pala, V.; Arbiol, A. Multiresolution-Based Image Fusion with Additive Wavelet Decompostion. IEEE Transactions on Geoscience and Remote Sensing **1999**, *37* (3), 1204–1211.
4. Abu-Rezq, A.N.; Tolba, A.S.; Khuwaja, G.A.; Foda, S.G. Best Parameters Selection for Wavelet Packet-Based Comparison of Magnetic Resonance Images. Computers and Biomedical Research **1999**, *32* (5), 449–469.
5. Ho, K.C.; Chan, Y.T. Optimum Discrete Wavelet Scaling and its Application to Delay and Doppler Estimation. IEEE Transactions on Signal Processing **1998**, *46* (9), 2285–2290.
6. Chen, V.C. Radar Ambiguity Function, Time-Varying Matched Filter, and Optimum Wavelet Correlator. Optical Engineering **1994**, *33* (7), 2212–2217.
7. Coifman, R.R.; Wickerhauser, M.V. Entropy-Based Algorithms for Best Basis Selection. IEEE Transactions on Information Theory **1992**, *38* (2), 713–718.
8. Ramchandran, K.; Vetterli, M. Best Wavelet Packet Bases in a Rate-Distortion Sense. IEEE Transactions on Image Processing **1993**, *2* (2), 160–175.
9. Wise, B.M.; Ricker, N.L.; Veltkamp, D.J.; Kowalski, B.R. A Theoretical Basis for the Use of Principal Component Models for Monitoring Multivariate Processes. Process Control and Quality **1990**, *1* (1), 41–53.

10. Kourti, T.; MacGregor, J.F. Process Analysis, Monitoring and Diagnosis, Using Multivariate Projection Methods. Chemom. Intell. Lab. Syst. **1995**, *28* (1), 3–21.
11. Wise, B.M.; Gallagher, N.B. The Process Chemometrics Approach to Process Monitoring and Fault Detection. J. Process Control **1996**, *6* (6), 329–348.
12. Jackson J.E. *A User's Guide to Principal Components*; John Wiley & Sons, Inc.: New York, 1991; 4–122.
13. Veltkamp, D.J. Multivariate Monitoring and Modelling of Chemical Processes Using Chemometrics. Process Control and Quality **1993**, *5* (2–3), 205–218.
14. Wenfu, K.; Strorer, R.H.; Georgakis, C. Disturbance Detection and Isolation by Dynamic Principal Component Analysis. Chemom. Intell. Lab. Syst. **1995**, *30* (1), 179–196.
15. Dunia, R.; Qin, S.J.; Edgar, T.F.; McAvoy, T.J. Use of Principal Component Analysis for Sensor Fault Identification. Comput. Chem. Eng. **1996**, *20* (Suppl. A), S713–S718.
16. Montgomery D.C. *Introduction to Statistical Quality Control*; John Wiley & Sons, Inc.: New York, 1996; 1–100.
17. Kosanovich, K.; Piovoso, M. PCA of Wavelet Transformed Process Data for Monitoring. Intell. Data Anal. **1997**, *1*, (http://www-east.elsevier.com/ida).
18. Stork, C.L.; Veltkamp, D.J.; Kowalski, B.R. Detecting and Identifying Spectral Anomalies Using Wavelet Processing. Applied Spectroscopy **1998**, *52* (10), 1348–1352.
19. Khashan, M.A.; El-Naggar, A.M.; Shaddad, E. A New Method of Determining the Optical Constant of a Thin Film from its Reflectance and Transmittance Interferograms in a Wide Spectral Range: 0.2–3 μm. Optics Communcations **2000**, *178* (1), 123–132.
20. Hart, M.; Vass, D.G.; Begbie, M.L. Fast Surface Profiling by Spectral Analysis of White-Light Interferograms with Fourier Transform Spectroscopy. Applied Optics **1998**, *37* (10), 1764–1769.
21. Ferrari, J.A.; Frins, E.; Rondoni, A.; Montaldo, G. Retrieval Algorithm for Refractive-Index Profile of Fibers from Transverse Interferograms. Optics Communications **1995**, *117* (1), 25–30.
22. Kim, H.J.; James, B.W. Two-Dimensional Fourier-Transform Techniques for the Analysis of Hook Interferograms. Applied Optics **1997**, *36* (6), 1352–1356.
23. Lyuboshenko, I. Unwrapping Circular Interferograms. Applied Optics **2000**, *39* (26), 4817–4825.

24. Paez, G.; Strojnik, M. Convergent, Recursive Phase Reconstruction from Noisy, Modulated Intensity Patterns by use of Synthetic Interferograms. Optics Letters **1998**, *23* (6), 406–408.
25. Yasuno, Y.; Nakama, M.; Sutoh, M.; Yatagai, T.; Mori, M. Phase-Resolved Correlation and its Application to Analysis of Low-Coherence Interferograms. Optics Letters **2001**, *26* (2), 90–92.
26. Recknagel, R-J.; Notni, G. Analysis of White Interferograms Using Wavelet Methods. Optics Communications **1998**, *148* (1), 122–128.

Received July 2, 2001
Accepted March 15, 2002